ISSN 2229-5518

A Simple Cloud Detection Algorithm Using NOAA-AVHRR Satellite Data

Radha Rani Ghosh, M. Shahjahan Ali, Ashrafunnahar Hena and H. Rahman

Abstract— *Detection of clouds and analysis of cloud frequency play an important role in operational weather prediction as well as in eco-climatological studies. In the present study, a threshold* based technique for cloud detection in Bangladesh and its surrounding areas has been developed based on National Oceanic and Atmospheric Administration Advanced Very High Resolution Radiometer (NOAA - AVHRR) satellite time-series data. The method consists of three tests. The first test is based on channel-1 reflectance of AVHRR images. The second test is based on channel-4 temperature of the same images. And the third test is based on both channel-1 and channel-4 data. Cloud detection is performed using the first and second test and the third test is used to detect cloud shadow. The algorithm has been applied to the NOAA-17 day time imagery for prominent seasons of Bangladesh for detecting clouds. Performance of the method has been evaluated visually. It is observed that the efficiency of the method in detecting cloudy pixels is sufficiently higher for operational use.

Index Terms— Cloud detection, NOAA-AVHRR, Threshold based technique, performance of cloud detection.

1 INTRODUCTION

CLOUD detection on the basis of data from geostationary or polar orbiting weather satellites has a long tradition in satellite meteorology [1], [2], [3]. Cloud information is especially important for now-casting purposes [4] and as an input for different satellite based estimation of atmospheric and surface parameters [5], [6], [7]. The spatial information on the occurrence of clouds, its frequency, types; phases as well as optical and microphysical properties are also of great importance for climatic-ecological studies [8], [9], [10], [11], [12], [13].

Clouds also play important role in the energy balance and the water cycle of the vegetation. As a result, the availability of cloud and rainwater determines the vertical distribution of vegetation [5]. Several cloud-classification schemes based on data from the polar and geostationary orbits have been developed in Europe and America over the last decades. Unsupervised classification by cluster analysis was developed by Seddon and Hunt, Guillory et al., and McClain et al. [14], [15], [16]. A successful strategy was to use one-dimensional and multidimensional histogram techniques [17]. The most common methods for cloud detection are the threshold-based algorithms which are based on NOAA-AVHRR data like APPOLO schemes [18], [19], [20] or supervised classification approaches like SCANDIA scheme of Karlson [21], [22]. The threshold technique is relatively simple. It applies several spectral and spatial tests to satellite data to detect not only cloud filled pixels but also the types of clouds. But there is problem related to threshold based technique- it is space sensitive and requires several adaptations to the threshold [5], [23].

The practice of utilization of modern space based technology to gather knowledge about the spatial pattern of clouds, cloud frequency and precipitation is rather low for Bangladesh, a country which is very much vulnerable to climate change. The goal of this study is to present a simple threshold based method for the detection of cloud in a tropical environment of Bangladesh and its adjacent areas from NOAA-AVHRR digital images.

2 DEVELOPMENT OF SATELLITE BASED ALGORITHM

A simple 4-step threshold method using visible and infrared channels was developed to detect the cloud contaminated pixels from NOAA-17/AVHRR visible and thermal infrared day-time imagery. Satellite visible (VIS) and infrared (IR) imagery have different ways of detecting clouds. Visible imagery is produced by the sun's rays reflecting off of clouds. Infrared imagery is produced by sensing the emitted radiation coming off of clouds. Temperature of cloud will determine the wavelength of radiation emitted from

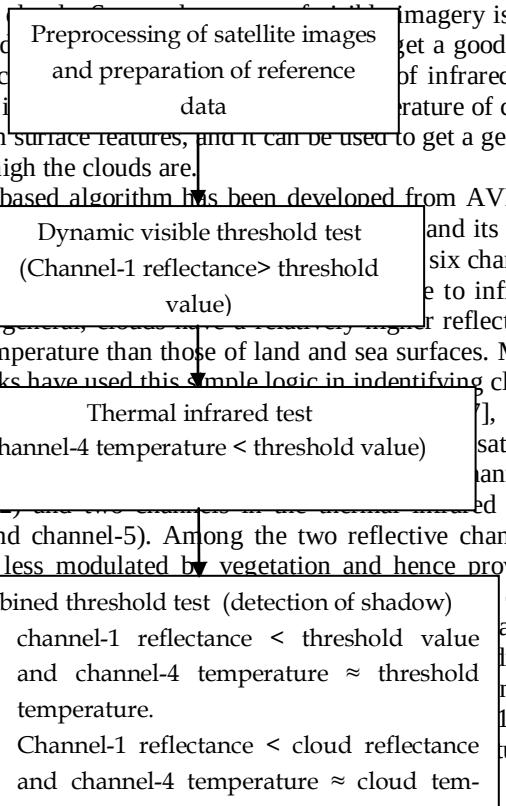

Fig. 1 Algorithm of cloud detection scheme.

The algorithm of the developed cloud detection scheme has been presented in figure-1.

Step 1: Preparation of clear sky reference layer- The orbiting satellites, like NOAA, provide images having swath width of about 2399 km. Due to such large swath width, during the scanning process, a number of geometric distortions are introduced into the image data [32]. Also, raw images obtained from the ground receiving stations are not maps. They could not be used to find positional parameter of any point on the image or for image to image comparison. Therefore, geometric correction of the images is necessary for achieving required locational accuracy and registering the images with a common map coordinate system. Also the images are radiometrically calibrated to convert the DN values to physical parameters; top of atmosphere (TOA) reflectance from channel-1 and brightness temperature from channel-4. Geometric correction and radiometric calibration have been done as described by [33] and [34] respectively. On the clear sky, the dominant element of the observed reflectance and brightness temperature are the ground reflectance and ground temperature respectively, which depend on the ground conditions and atmospheric conditions, such as moisture content and vegetation.

At first, in order to detect cloud-contaminated pixels by Channel-1 for various ground conditions, a reference ground reflectance map should be prepared. Since the ground reflectance is much lower than cloud reflectance and that the lifetime of cloud is generally shorter, it is proposed that the minimum value of the reflectance derived at a certain site within a certain period of time can be taken as the signature of the reference ground reflectance [35]. We have constructed the clear sky ground reflectance image layer using a simple filtering method applied to the time series of satellite images; in this case, all daytime images (apparently cloud free images only) for a month. All images for the month under analysis were compared, and minimum values for the corresponding pixels were taken. The minimums of these apparent values for a month were retained as the clear sky reference reflectance of the pixels for the month [36]. Here reference reflectance contains the reflectance of the surface plus the reflectance from a clean, clear and dry atmosphere above the surface. Secondly, in order to detect cloud-contaminated pixels by channel-4 on various thermal conditions, a reference brightness temperature image of the ground should be prepared. Since the brightness temperature of ground is higher than the brightness temperature of cloud, the minimum value of the brightness temperature derived at a certain site within a certain period of time can be taken as the index of the reference ground temperature [35]. The reference ground temperature map has been prepared using the same procedure for preparation of reference ground reflectance map.

Step 2: Dynamic Visible Threshold Test - The first test for cloud detection is the dynamic visible threshold test using TOA reflectance value from channel-1. The threshold value is identified from the reference ground reflectance. In this test, all pixels with channel-1 reflectance greater than a predefined threshold value are defined as cloudy [37].

Step 3: Thermal Infrared Test- The second test is the threshold temperature test using brightness temperature from channel-4. In this test, all pixels with brightness temperature less than a predefined value are taken as cloudy. Both the visible test and thermal test can be used to detect all cloud types.

Step 4: Combined Threshold Test (Ch-1 & Ch-4) - The purpose of this test is to detect shadow of cloud on earth surface and shadow of one cloud on another cloud. When shadow is cast by clouds on earth surface, the reflectance of the surface covered by shadow becomes lower than the clear sky reflectance of the area but the temperature of the surface does not change noticeably between the clear and shadow cases. On the other hand, when shadow is occurred by one cloud on another cloud, its reflectance become much lower than the cloud reflectance and temperature remains the same as the cloud. Thus the shadow on ground and on the cloud can be detected through the combined reflectance and temperature test.

3 RESULT AND DISCUSSION

The algorithm developed in this study was tested for full resolution AVHRR/3 images from day-time NOAA-17 passes over

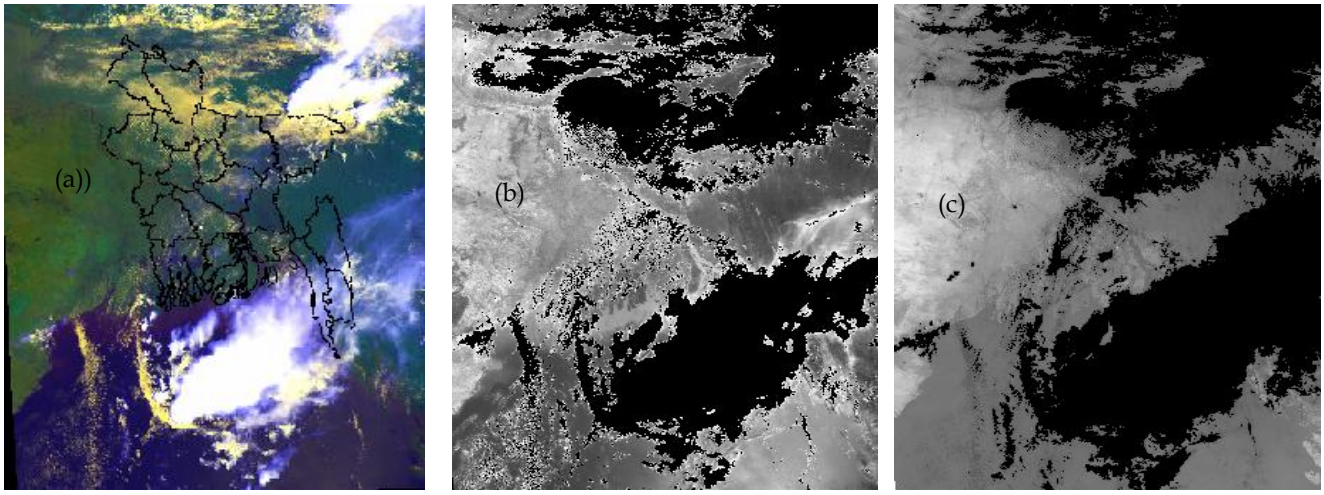

Fig. 2 (a) Raw multispectral image of 15 April 2005, 10:35am. (b) Monochrome image showing cloud areas obtained through test-1 and (c) Image showing cloud areas obtained through test-2.

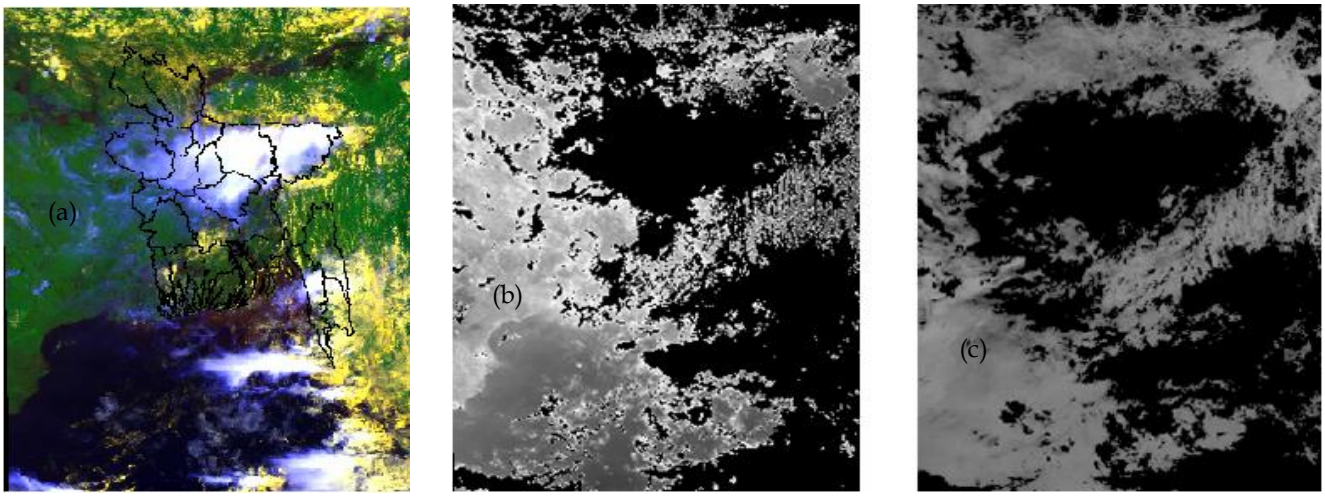

Fig. 3 (a) Shows the raw satellite image of 02 August 2005 11:05am. (b) Image showing cloud areas through test-1 and (c) Image showing cloud areas obtained through test-2.

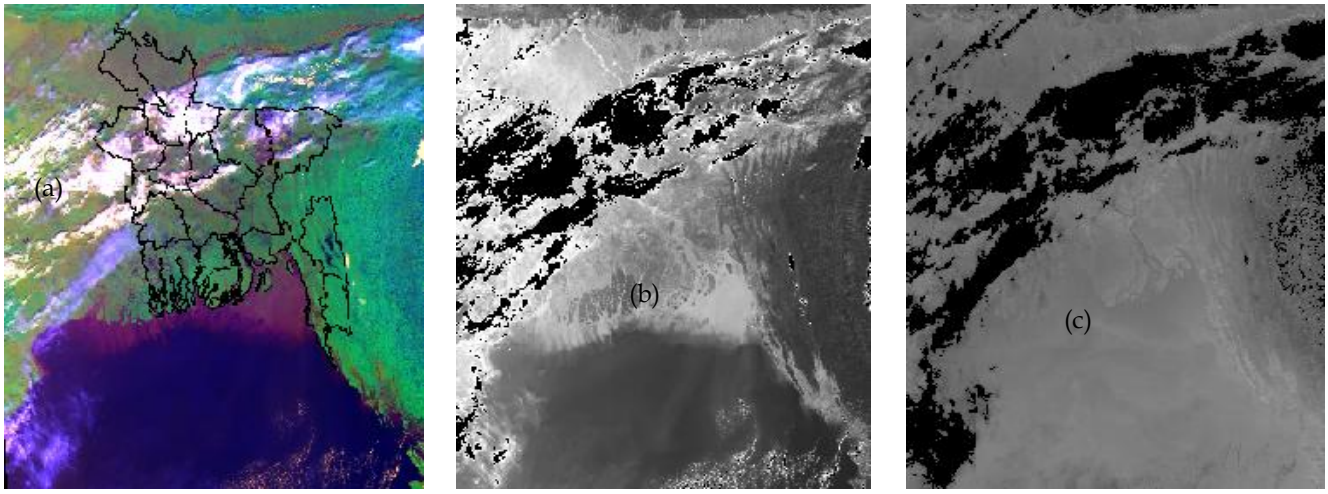

Fig. 4 (a) Shows the raw satellite image of 17 December 2005, 10:00am. (b) Image showing cloud areas through test-1 and (c) Image showing cloud areas obtained through test-2

Bangladesh and its adjoining areas. Data for the months of April, August and December for the year 2005 was processed for this study. The images were obtained from satellite Earth station located at Bangladesh Space Research and Remote Sensing Organization (SPARRSO). The data were first Earth-located and calibrated to obtain brightness temperatures and top-of-atmosphere bidirectional reflectances required as input to the cloud detection scheme. In the present technique, three threshold tests were applied to the day-time AVHRR data for the detection of cloud-contaminated pixels. Efficiency of the algorithm in detecting clouds was assessed through visual inspection between raw multispectral color images and corresponding cloud masked images (single channel black and white image). Seasonal variations of threshold values were determined by taking images from three prominent seasons (winter, summer and monsoon) of Bangladesh.

Fig 2(a) shows the raw image of 15 April 2005 (summer period). The time of satellite pass was 10:35am local standard

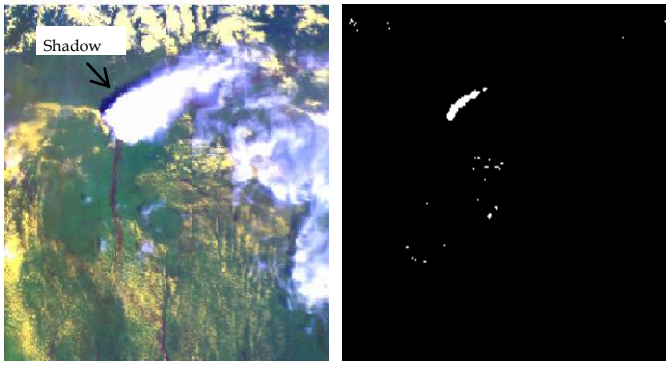

Fig. 5 Shadow cast by cloud on Earth's surface (left). In the right, shadow detected by using the combined application of the reflectance and temperature properties.

time (LST). For this month the threshold reflectance and threshold brightness temperature values were 20% and 18°C respectively. Figure 2(b) and figure 2(c) present the resulting images after performing test-1 (reflectance test) and test-2 (temperature test) respectively. In Fig. 2(b) the image features whose reflectances are higher than 20% have been marked as clouds. In Fig. 2(c) features whose temperatures are lower than 18°C have been classified as clouds. The cloudy pixels are shown in black.

Fig 3(a) shows the satellite image of 02 August 2005 (rainy season). The time of image acquisition was 11:05am LST. For this month the threshold reflectance and threshold temperature values were 15% and 10°C respectively. Figure 3(b) and figure 3(c) present the cloud masked images obtained by performing test-1 and test-2 respectively.

A raw image contains some cloud of 17 December 2005 (winter season) is shown in Fig. 4(a). The time of image acquisition was 10:00am LST. For this month, the threshold reflectance and threshold brightness temperature values were 19% and 14°C respectively. Fig. 4(b) and Fig. 4(c) present the cloud maps obtained through applying test-1 and test-2 respectively.

Fig. 5(a) shows a typical satellite image containing shadow casts by cloud on the Earth's surface. The image was received on 23 Aril 2005 at 11:10am. Fig. 5(b) presents the image of cloud shadow marked by the combined application of reflectance and temperature test. White areas in this image represent the cloud shadow.

From the study it is observed that the reference values of reflectance and temperature vary with seasonal variations. Also there is a small difference in the ways the two threshold based algorithms perform cloud detection functions. A small under- and over-estimation problem has been witnessed for both the tests. From the images as depicted in Fig. 2(a) to 2(c) it is observed that, for summer periods, both the reflectance and temperature based tests have reasonably higher efficiency in identifying cloudy pixels. Dynamic visible threshold test, however, cannot detect a small number of very thin water-cloud pixels as observed in the middle-right part of figure-2(b). This may happen due to the fact that reflectance of the very thin water clouds may sometimes be equal to or even sometimes lower than the cloud-free land surfaces and so this type of clouds were flagged as clear pixels. By inspecting the images from Fig. 3(a) to Fig. 3(c) it is observed that, for monsoon period, test-1can detect all types of clouds with higher efficiency but test-2 cannot detect many of the low-level broken clouds as seen in the upper part of Fig. 3(c). This shortcoming of temperature based test may arises from the fact that the average temperature of the lower height broken cloud pixels may be very close to that of cloud free surfaces. For winter period it is observed that efficiency of test-2 (thermal infrared test) is higher than that of test-1 in identifying all cloud types [Fig. 4(a) to 4(c)]. In case of test-1 some of the pixels originally covered by thin low level clouds remain undetected as seen in the top-right part of Fig. 4(b). Saunders and Kriebel [19] reported similar results of channel properties when applying multispectral AVHRR data to detect cloud.

4 Conclusion

In this study, a threshold technique has been developed to detect cloud for a tropical region. The method is consists of three tests to detect cloud and cloud shadow using AVHRR radiometer data from the polar orbiter NOAA satellite. The efficiency of the method in identifying clouds was tested visually. It was observed that the method can detect almost all of clouds with reasonable accuracy. It was also observed that there are some seasonal effects on the effectiveness of the visible and thermal infrared tests.

Acknowledgment

The authors gratefully acknowledge the administrative support and satellite data provided by the Bangladesh Space Research and Remote Sensing Organization (SPARRSO), Dhaka.

References

[1] Stowe, L.L., R. McClain, R. Carey, P. Pellegrino, G.G. Gutman, P. Davis, C.Long, and S.Hart. 1991. Global distribution of cloud cover derived from NOAA/AVHRR operationalsatellite data. *Advances in Space Research* **3**, 51-54.

[2] Hamil T.M., R.P. d'Entremont and J.T. Bunting, 1992. A description of the Air Force real-time nephanaanalysis model, *Wea. And Fcst*., **7**, 288-306.

[3] Rossow W.B., and L.C. Garder, 1993 Cloud detection using satellite measurements of infrared and visible radiances for ISCCP. *Journal of climate*, **6**, 2341-2369.

[4] Stephens G.L., G. Vane, R.J. Boain, G.G. Mace, K. Sassen, Z. Wang, A.J. Illinworth, E.J. O□Conner, W.B. Rossow, S.L.Durden, S.D. Miller, R.T. Austin, A. Benedetti, C. Mitrescu. The cloud Sat Science Team 2002: The CloudSat mission and the A-Train, *Bull. Amer. Meteor. Soc.*, **83(12)**, 1771-1790.

[5] Bendix J., R. Rollenbeck and W.E. Palacios, 2004. Cloud detection in the Tropics- a suitable tool for climate-ecological studies in the high mountains of Equador. *Intl. J. Rem. Sens*., **25** (21), 4521-4540.

[6] Albers S.C., J.A. McGinley, D.A.Birkenheuer and J.R. Smart 1996. The local analysis of prediction system (LAPS): Analysis of clouds, precipitation and temperature. *Wea. Forcasting*, **11**, 273-287.

[7] Sandvik A.D., 1998. Implementation and validation of a condensation scheme in a messoscale model. *Mon. Sea. Rev*., 126, 1882-1905.

[8] Weilicki, B.A., B.R. Barkstrom, E.F. Harrison, R.B. Lee III, G.L. Smith and J.E. Cooper 1996. Clouds and the Earth's Radiant Energy System (CERES); An Earth Observing system experiment, *Bull. Amer. Meteorol. Soc*., **77,** 853-868.

[9] Mitchel J.F.B., 1989. The 'greenhouse effect' and climate change. Rev. Geophysic., **27**, 115-139.

[10] Jolivet, D. and A.J. Feijt, 2003. Cloud thermodynamic phase and particle size estimation using the 0.67 and 1.6 µm channels from meteorological satellites. *Atmos. Chem. Phys. Discuss.*, **3,** 4461-4488.

[11] Intergovernmental Panel on Climate Change (IPCC): Third Assessment Report. Watson R.T. and Coauthors, Cambridge University Press, New York, 398pp.

[12] van Meijgaard, E., L. H. van Ulft, W. J. van de Berg, F. C. Bosveld, B. J. J.M. van den Hurk, G. Lenderink, and A. P. Siebesma (2008), The KNMI-regional atmospheric climate model, version 2.1, KNMI Tech. Rep. 302,R. Neth. Meteorol. Inst., De Bilt, Netherlands.

[13] Woick H., J. Schmetz and S. Tjemkes, 1997. An introduction to METEOSAT second generation imagery and products. Proc. of th e1997 UMETSAT Meteorological Satellite Data User's Conference, Brussels, UMETSAT, Darmstad, 395-400, 1997.

[14] Seddon A.M. and G.E. Hunt, 1985. Segmentation of clouds using cluster analysis, *Int. J. Remote Sens*., **6**, 717-731.

[15] Guillory A.R., J.M. Lecue, G.J. Jedlovec and B.N. Whitworth (1998). Cloud filtering using a bi-spectral spatial coherence approach. 9th Conference on satellite meteorology and oceanography, AMS, Paris, France, pp 374-376.

[16] McClain E.P, W.G. Pichel and C.C Walton (1985). Comparative performance of AVHRR based multichannel sea surface temperatures. *J. Geophys. Res.*, **90**, 11587- 11601.

[17] Desbois M., G. seze, G. Szejwach, 1982. Automatic classification of clopuds on METEOSAT imagery: Application to higholevel clouds, *J. App. Meteorology*, **21**, 401-412.

[18] Saunders R.W. (1986). An automated scheme for the removal of cloud contamination from AVHRR radiances over western Europe. *Int. J. Remote Sen.,* **7**, 867-886.

[19] Saunders R.W. and Kriebel K.T. (1988) An improved method for detecting clear shy and cloudy radiances from AVHRR data. *Int. J. Remote sensing*, **9(1)**, 123-150.

[20] Kribel K.T. G Gesell, M. Kastner and H. Mannstein (2003). The cloud analysis tool APOLLO: Improvements and validations. *Int. J. Remote Sens*., **24**, 2389-2408.

[21] Karlson K.G. (1989). Development of an operational cloud classification model. *Int. J. Remote Sens.,* **10**, 687-693.

[22] Karlson (1996). Cloud classification with the SCANDIA model. *Swedish Meteorological and Hydrological Institute Rep. of Meteorology and Climatology*. **67**, 36 pp.

[23] Hutchison K.D., and K.R. Hardy 1995. Threshold functions for automated cloud analysis of global meteorological satellite imagery. *Int. J. Remote. Sen.*, **16**, 3665-3680.

[24] Reynolds, D.W and T.H. Vonder Haar, 1977, A bi-spectral method for cloud parameter deterination. *Mon. Wea. Rev*., **105**, 446-457.

[25] Schiffer, R.A. and W.B. Rossow, 1983, The ISCCP: The first project of the world climate research programme. *Bull. Amer Meteor. Soc*., **64**, 779-784.

[26] Chou S.H., D. Atlas and E.N. Yeh, 1986. Turbulence in a convective marine atmosphere boundary layer. *J. Atmos. Sci.,* **43,** 547-564.

[27] Seze, G. and M. Desbois, 1987, Cloud cover analysis from satellite imagery using spatial and temporal characteristics of the data. *J. Climate Appl. Meteor*., **26,** 287-303.

[28] Derrien M., B. Farki, L. Harang, H. LeGleau, A. Noyalet, D. Pochic and A. Sairouni, 1993, Automatic cloud detection applied to NOAA-11/AVHRR imagery. 46, 246-267.

[29] Kriebel K.T., G. Gesell, M. Kastner, and H. Mannstein, 2003. The cloud analysis tool APPOLO: improvements and validations. *Int. J. Rem. Sen*., **24**, 2389-2408.

[30] Suh, M.S., and K.Y. Park, 1993, Cloud cover analysis from GMS/S-VISSR imagery using bispectral thresholds technique. *J. Korean Soc. Remote Sensing*, **9,** 1-19.

[31] Pinheiro A.C.T., R. Mahoney, J.L. Privette, C.J. Tucher, 2006. Development of a daily long term record of NOAA-14 AVHRR land surface temperature over Africa. *Remote Sensing of Environment*, **103**, pp 153-164.

[32] Sabins Floyd F. Jr., Remote Sensing: Principles and Interpretation, pp 246-248, W. H. Freeman and Company, San Francisco, USA, 1996.

[33] Ali M.S., H. Rahman and R.K. Mazumder, 2007. Geometric correction of NOAA-AVHRR satellite images for solar radiation applications. J. *Bangladesh Electron. Soc*., **7(1-2)**, 87-90.

[34] Planet, W.G., 1988, Data extraction and calibration of Tiros-N/NOAA radiometers, NOAA Technical Memorandum NESS 107, Washington, D.C.

[35] Otani K., I. Suda, K. Kuroka, In-Proceedings of ASEAN Energy Technology Conference, 28-29 August, 1995, pp 306-312.

[36] Islam M.R. and R.H.B. Excell, 1996. Solar radiation mapping from satellite images using a low cost system. *Solar energy*, **56(3)**, 225-237.

[37] Kubota M. (1994). A new cloud detection Algorithm for Nighttime AVHRR/HRPT. *Journal of Oceanography*, **50**, 31-41.